






RESEARCH ARTICLE | FEBRUARY 05 2025

Rheology of mRNA-loaded lipid nanodumbbells

Special Collection: [Flow and Lipid Nanoparticles](#)

Mona A. Kanso (منى قانسو) ; Shalini Singh (शालिनी सिंह) ; Alan J. Giacomini ; Richard D. Braatz  



Physics of Fluids 37, 023109 (2025)

<https://doi.org/10.1063/5.0251449>



Articles You May Be Interested In

Lopsided elastic dumbbell suspension

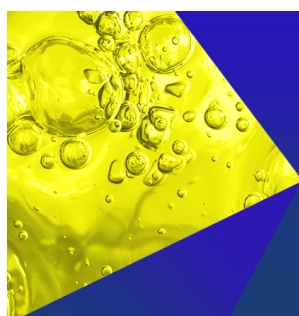
Physics of Fluids (July 2024)

Lopsided rigid dumbbell rheology from Langevin equation: A graduate tutorial

Physics of Fluids (September 2024)

Carrier transfer induced photoluminescence change in metal-semiconductor core-shell nanostructures

Appl. Phys. Lett. (April 2006)



Physics of Fluids
Special Topics
Open for Submissions

[Learn More](#)



Rheology of mRNA-loaded lipid nanodumbbells

Cite as: Phys. Fluids **37**, 023109 (2025); doi: [10.1063/5.0251449](https://doi.org/10.1063/5.0251449)

Submitted: 2 December 2024 · Accepted: 20 December 2024 ·

Published Online: 5 February 2025







View Online



Export Citation



CrossMark

Mona A. Kanso (منى قانسو),¹  Shalini Singh (शालिनी सिंह),¹  Alan J. Giacomin,²  and Richard D. Braatz^{1,a)} 

AFFILIATIONS

¹Chemical Engineering Department, Massachusetts Institute of Technology, Cambridge 02139, USA

²Mechanical Engineering Department, University of Nevada, Reno, Nevada 89557-0312, USA

Note: This paper is part of the special topic, Flow and Lipid Nanoparticles.

^{a)}Author to whom correspondence should be addressed: braatz@mit.edu

ABSTRACT

In one important chemical engineering unit operation of messenger ribonucleic acid (mRNA) vaccine manufacture, the precious mRNA payload is encapsulated in lipid nanoparticles (LNPs). Recent elegant cryogenic-transmission electron microscopy [Brader *et al.*, Biophys. J. **120**, 2766 (2021)] reveals that these lipid nanoparticles take the form of dumbbell suspensions. When encapsulating their mRNA payloads, these dumbbells can be both lopsided and interpenetrating, with the smaller of the two beads carrying the payload. In this work, we arrive at analytical expressions for these suspensions of lopsided lipid nanoparticle dumbbells encapsulating mRNA payloads. For this, we first exploit rigid dumbbell theory [Abdel-Khalik and Bird, Appl. Sci. Res. **30**, 268 (1975)], which relies on the orientation distributions of the lopsided dumbbells, to predict the suspension rheology, and specifically to predict how this departs from Newtonian behavior. We next exploit elastic dumbbell theory [Phan-Thien *et al.*, Phys. Fluids **36**, 071707 (2024)], which also relies on the orientation distributions of the lopsided dumbbells and to which we add dumbbell stretching. Our results include analytical expressions for the relaxation time, rotational diffusivity, zero-shear viscosity, shear stress relaxation function, steady-shear viscosity and both the viscous part and *minus* the elastic part of the complex viscosity. We determine the rotational diffusivity of the mRNA-loaded lipid nanoparticle nanodumbbells from small-amplitude oscillatory shear measurements.

Published under an exclusive license by AIP Publishing. <https://doi.org/10.1063/5.0251449>

I. INTRODUCTION

In a vital step of mRNA vaccine production, the valuable messenger ribonucleic acid (mRNA) payload is encapsulated in lipid nanoparticles. Recent elegant cryogenic-transmission electron microscopy^{1–5} reveals these lipid nanoparticles take the form of nanodumbbell suspensions. These nanodumbbells are disperse. Their lengths differ broadly, and so do their bead diameters, and so does their lopsidedness.⁵ Moreover, their lipid nanoparticle shapes are also distributed, with some nanospheres, and other more exotic planar configurations involving three or four separate encapsulations.⁵

When encapsulating their mRNA payloads, the nanodumbbells can be both lopsided and interpenetrating, with the smaller of the two beads carrying the payload. In this work, we arrive at analytical expressions for these suspensions of lopsided lipid nanoparticle dumbbells encapsulating mRNA payloads. For this, we exploit both (i) rigid dumbbell theory,⁶ and (ii) elastic dumbbell theory.^{7,8} Romanette (i) relies on the orientation distributions of the lopsided dumbbells to predict the suspension rheology, and specifically to predict how the nanodumbbell orientation causes these suspensions to depart from Newtonian behavior. Romanette (ii) also relies on the orientation

distributions of the lopsided dumbbells to which Hookean dumbbell stretching is added. The Hookean dumbbell thus offers the prospect of exploring the role of mRNA lipid nanodumbbell extensibility on the rheology of their suspension. While Hookean dumbbells can lengthen and shorten, they can neither twist nor bend.

Our results include analytical expressions for the relaxation time, rotational diffusivity, zero-shear viscosity, shear stress relaxation function, steady-shear viscosity, and both the viscous part and *minus* the elastic part of the complex viscosity.

Whereas the preferred morphology for the vaccine might be mRNA encapsulated in a spherical lipid nanosphere,⁹ the predominant morphology is the nanodumbbell.⁵ Why this is so is not understood. The lopsidedness of the nanodumbbells may be due to the anionic payload and cationic lipid encapsulants. If so, the more lopsided the nanodumbbell, the more mRNA strands its blebs will contain. This hypothesis should be tested. It is known that, in practice, the average number of mRNA encapsulations per lipid nanoparticle is not a single count but ranges between 3 and 5.¹⁰

In the precipitation step of mRNA vaccine manufacture, mRNA is encapsulated in lipid nanoparticles.² This encapsulation stabilizes

the mRNA and packages it for vaccine delivery.¹¹ Detailed cryo-electron microscopy or atomic force microscopy of these encapsulations reveals dumbbell-shaped nanoparticles, with one bead of the dumbbell containing the mRNA payload and the other bead empty (Fig. 3 of Ref. 2; Figs. 1 and 2 of Ref. 1; upper right and lower left of Fig. 1 of Ref. 3; Fig. 2BC of Ref. 4; Fig. 3.a of Ref. 5; Fig. 2 of Ref. 12; Fig. 5.c of Ref. 39). We call these encapsulates *nanodumbbells*, whose shapes are described by three dimensions: two bead diameters, (i) one for the payloaded bead, d_p , and (ii) another for the other, d_b , and (iii) the length between these bead centers, L . The payloaded bead is usually smaller than the other

$$d_p < d_b, \quad (1)$$

and the two beads normally interpenetrate:

$$L < \frac{1}{2}(d_p + d_b). \quad (2)$$

When Eq. (1) holds, the dumbbell is said to be *lopsided*,^{6–8} as illustrated in Figs. 1–3. Since the mRNA encapsulate is not dragged

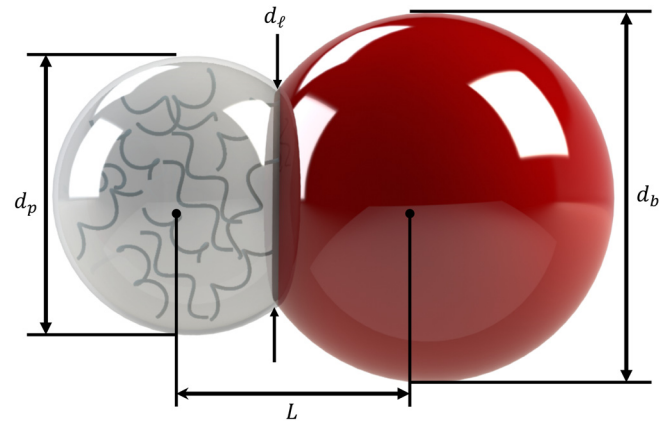


FIG. 2. Characteristic dimensions of predominant morphology [Panel (b) of Fig. 1], interpenetrated lopsided dumbbell lipid nanoparticle. The center-to-center distance, L , bead devoid of payload diameter, d_b , payload bead diameter, d_p and waistline diameter, d_l . For this example, $d_p/d_b = 4/5$, and $L/d_p = 9/10$.

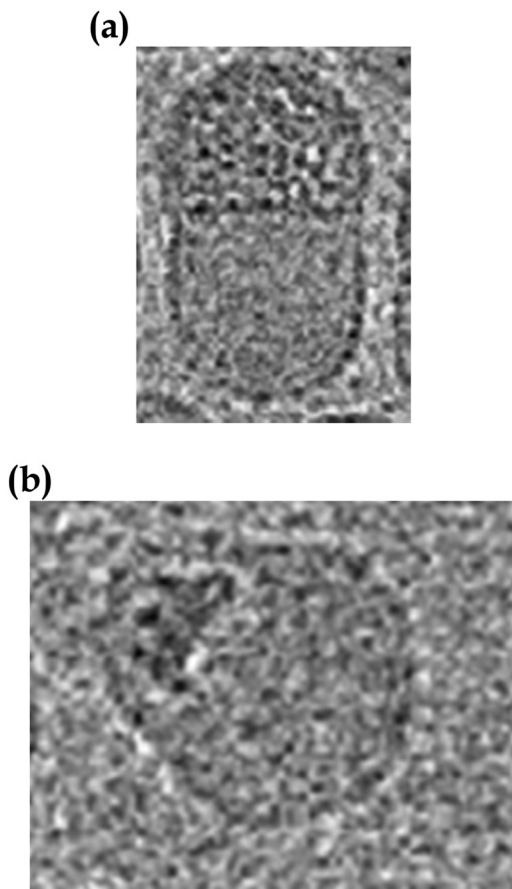


FIG. 1. Representative cryogenic-transmission electron micrography of (a) symmetric and (b) predominant morphology of payloaded LNP nanodumbbell (from Fig. 3 of Ref. 2). Figure 2 models (b). Reproduced with permission from Brader *et al.*, Biophys. J. **120**, 2766–2770 (2021). Copyright 2021 Elsevier (Cell Press).



FIG. 3. Isometric view of model of Fig. 2.

through fluid (see Fig. 3), it does not contribute to resisting reorientation of the lopsided dumbbell. We call this exclusion *screening* (see Sec. 13.7 of Ref. 13 and also Ref. 14). When both Eqs. (1) and (2) hold, the payloaded bead is called a *bleb*. If the interpenetrating payloaded bead is much smaller than its counterpart (say, $d_p \lesssim \frac{3}{4}d_b$), the bleb is called a *blister*. We find these important lipid nanodumbbell suspensions to be intrinsically beautiful, and we devote this paper to deriving expressions for their transport properties from general rigid bead-rod theory (also called rotarance theory). Tables I and II define, respectively, the symbols used herein, dimensional and dimensionless.

In macromolecular theory, even within the same chapter of textbooks, the word *lopsided* is used in two completely different ways. In the context of dumbbell suspension theory, lopsided means that one bead differs from the other [Eq. (1); row 2 of Table XIII.IV-I of Ref. 13 and row 2 of Table XVI.IV-I of Ref. 15]. By contrast, in the context of rotarance theory, lopsided means something entirely different. In this context, lopsided means that the moment of inertia of the

TABLE I. Dimensional variables. Legend: $M \equiv$ mass, $L \equiv$ length, $t \equiv$ time.

Name	Dimension	Symbol
Angular frequency	t^{-1}	ω
Bead diameter	L	d
Bead diameter, payloaded	L	d_p
Bead diameter, without payload	L	d_b
Bead friction coefficient, lopsided dumbbell, payloaded	M/t	ζ_p
Bead friction coefficient, lopsided dumbbell, without payload	M/t	ζ_b
Bead friction coefficient, symmetric dumbbell	M/t	ζ
Bead mass, without payload	M/bead	m_b
Bead mass, payloaded	M/bead	m_p
Boltzmann constant	ML^2/t^2T	k
Concentration	dumbbells/ L^3	n
Diameter, waistline, symmetric dumbbell	L	d_i
Diameter, waistline, lopsided dumbbell	L	d_ℓ
Dirac delta function of time	t^{-1}	$\delta(t)$
Length, dumbbell, center-to-center	L	L
Mass concentration	M/L^3	c
Moments of inertia, dumbbell	ML^2	I_3, I_2, I_1
Relaxation time, lopsided rigid dumbbell	t	λ_ℓ
Relaxation time, symmetric Hookean elastic dumbbell	t	λ_H
Relaxation time, symmetric rigid dumbbell	t	λ
Rotational diffusivity, lopsided rigid dumbbell	t^{-1}	$D_{r\ell}$
Rotational diffusivity, symmetric rigid dumbbell	t^{-1}	D_r
Shear rate, steady	t^{-1}	$\dot{\gamma}$
Shear relaxation function	M/Lt^2	$G(s)$
Stiffness, lipid shell	M/t^2	k
Stiffness, lipid shell, payloaded	M/t^2	k_p
Stiffness, lipid shell, without payload	M/t^2	k_b
Spring stiffness	M/t^2	H
Surface area, lopsided dumbbell	L^3	S_ℓ
Surface area, symmetric dumbbell	L^3	S
Temperature, absolute	T	T
Thickness, lipid shell	L	h
Thickness, lipid shell, payloaded	L	h_p
Thickness, lipid shell, without payload	L	h_b
Time	t	t
Viscosity, complex, <i>minus</i> imaginary part	M/Lt	$\eta''(\omega)$
Viscosity, complex, real part	M/Lt	$\eta'(\omega)$
Viscosity, steady shear	M/Lt	$\eta(\dot{\gamma})$
Viscosity, zero-shear	M/Lt	η_0
Volume, lopsided dumbbell	L^3	V_ℓ
Volume, symmetric dumbbell	L^3	V
Young's modulus	M/Lt^2	E
Young's modulus, lipid shell, payloaded	M/Lt^2	E_p
Young's modulus, lipid shell, without payload	M/Lt^2	E_b

macromolecule about the molecular axis divided by the moment about either transverse axis is not one, that is, that $I_3/I_1 \neq 1$ or that $I_3/I_2 \neq 1$. Otherwise put, in rotarance theory, lopsided means not spherically symmetric. For dumbbells, be they lopsided or not, $I_3/I_1 =$

0 (example 13.6–1 of Ref. 13; example 16.7–1 of Ref. 15; see also Eq. (3) in Ref. 16). In this paper, going forward, *lopsided* always means one bead differing from the other, and specifically, $d_b/d_p > 1$. Therefore, lopsidedness in the context of dumbbell suspension theory

16 March 2025 02:58:42

TABLE II. Dimensionless variables and groups.

Name	Symbol
Deborah number, lopsided	$\lambda_\ell \omega$
Deborah number, symmetric	$\lambda \omega$
Dimensionless surface area, lopsided dumbbell	S_ℓ/V
Dimensionless volume, lopsided dumbbell	V_ℓ/V
Lopsidedness, rigid dumbbell sense	d_b/d_p
Lopsidedness, rigid dumbbell sense, viscosity average	\bar{d}_b/\bar{d}_p
Perimeter, beads, symmetric dumbbell (waistline)	d_ℓ/d_i
Perimeter, bleb, lopsided dumbbell (waistline)	d_ℓ/d_i
Poisson ratio ($\nu = 0.5$)	ν
Subscript, indicating lopsided	ℓ
Weissenberg number, lopsided	$\lambda_\ell \dot{\gamma}$
Weissenberg number, symmetric	$\lambda \dot{\gamma}$

is not to be confused with lopsidedness in the context of rotarance theory.

From the available cryo-electron micrography (Fig. 3 of Ref. 2; upper right and lower left of Fig. 1 of Ref. 3; Fig. 2BC of Ref. 4; Fig. 3a of Ref. 5), of the mRNA lipid nanodumbbells, the approximate dimensions are

$$29 \lesssim L \lesssim 42 \text{ nm}, \quad (3)$$

$$38 \lesssim d_b \lesssim 63 \text{ nm}, \quad (4)$$

$$20 \lesssim d_p \lesssim 54 \text{ nm}, \quad (5)$$

and the dimensionless lopsideness

$$1 \lesssim \frac{d_b}{d_p} \lesssim 2 \quad (6)$$

dispersities in mRNA nanodumbbell encapsulations. The end-to-end distance of a lopsided nanodumbbell is thus $[L + \frac{1}{2}(d_b + d_p)]$, which is of course longer than the center-to-center distance.

Since nanodumbbells are longer than they are wide, each has one and only one orientation. These orientations affect profoundly the particle transport properties. The orientation distribution function imparts a relaxation time to the dumbbell suspension, a rotational diffusivity to the particles and a particle contribution to the rheological properties. For dumbbell suspensions of orientable particles, we can arrive at expressions for the transport properties both analytically, and from first principles. We do so in two steps.

For rigid dumbbells, we first formulate the conservation of orientation (called the diffusion equation) in spherical coordinates and solve it for the orientation distribution function.¹⁷ This step yields the relaxation time, and the rotational diffusivity of the particle suspension. Second, we use the orientation distribution to determine the stresses in a well-defined flow.¹⁷ For instance, in simple shear performed at low-shear rate, we get the zero-shear viscosity. Arrived at in these ways, for symmetric dumbbells, where $d_p = d_b$, many material functions are well-known. In this paper, we will focus on four of these: (i) the zero-shear viscosity, (ii) the steady shear viscosity,¹⁸ and (iii) both parts of the complex viscosity.

For Hookean elastic dumbbells, we first formulate the conservation of orientation (called the diffusion equation) in spherical coordinates and solve it for the configuration distribution function

(Chapter 13 of Ref. 15). This step yields the relaxation time, and the rotational diffusivity of the particle suspension (based on the Hookean elastic dumbbell suspension). Second, we use the configuration distribution to determine the stresses in a well-defined flow (Chapter 13 of Ref. 15).

For rigid dumbbell suspensions, the equations for most canonical rheological material functions are known. This rich and growing literature includes (iv) superposition of steady shear flow and small-amplitude oscillatory shear flow (both parallel and transverse [Eqs. (8.16)–(8.18) and (22.8)–(22.9) of Refs. 26 and 19], (v) large-amplitude oscillatory shear flow;^{20–25} [Eqs. (9.3)–(9.4) of Ref. 26], (vi) stress relaxation following cessation of steady shear flow [Eqs. (10.6)–(10.8) of Ref. 26], (vii) stress growth following sudden inception of steady shear flow [Eqs. (11.8)–(11.10) of Ref. 26], (viii) constrained recoil after cessation of steady shear flow [Eqs. (12.16), (12.19)–(12.20) of Refs. 26 and 27], (ix) shear creep [Eqs. (13.16)–(13.17) of Refs. 26 and 28], (x) stress growth following shear rate ramp [Eq. (14.5) of Ref. 26], (xi) steady uniaxial or equibiaxial elongation [Eqs. (16.5)–(16.6) of Ref. 26], (xii) stress relaxation following cessation of steady uniaxial or equibiaxial elongation [Eqs. (17.8)–(17.9) of Ref. 26], (xiii) the steady planar extensional viscosities [Eqs. (64)–(65) of Ref. 29] or to conveniently combine Eqs. (31)–(32) of Ref. 30 with the bridge from continuum to macromolecular theory [Eqs. (21)–(23), (27)–(29), (32)–(33) of Ref. 31], (xiv) stress relaxation following inception of steady uniaxial or equibiaxial elongation [Eqs. (18.9) of Ref. 26], (xv) recoil after cessation of steady uniaxial or equibiaxial elongation [Eq. (19.14) of Ref. 26], and (xvi) eccentric rotating disk flow [Eqs. (21.6)–(21.7) of Refs. 26 and 32]. For elastic Hookean dumbbells suspensions, the equations for most canonical rheological material functions are also known (Chapter 13 of Ref. 15). For polymeric liquids, the rigid dumbbell suspension agrees with the measured rheological behaviors, and the Hookean dumbbell does not. For suspensions of lopsided mRNA nanodumbbell suspensions, the verdict is still out. We devote this paper to this topic.

For instance, the dumbbell contribution to the zero-shear viscosity of a symmetric dumbbell suspension is [Eq. (6.7) of Ref. 26]

$$\eta_0 - \eta_s = nkT\lambda. \quad (7)$$

The steady shear viscosity [Eq. (6.7) of Ref. 26] is

$$\frac{\eta(\dot{\gamma}) - \eta_s}{\eta_0 - \eta_s} = 1 - \frac{18}{35}(\lambda\dot{\gamma})^2 + \frac{1326}{1925}(\lambda\dot{\gamma})^4 + \dots \quad (8)$$

The stress relaxation function following step shear [Eq. (11) of Ref. 34 with row 1 of Table XV. of Ref. 34 in which we set $N = 2$] is

$$G(t) = \left(2\eta_s + \frac{4}{5}nkT\lambda\right)\delta(t) + \frac{3}{5}nkTe^{-t/\lambda}, \quad (9)$$

and the viscous and elastic parts of the complex viscosity [Eq. (7.17) of Ref. 26] are

$$\frac{\eta'(\omega) - \eta_s}{\eta_0 - \eta_s} = 1 - \frac{3}{5} \frac{(\lambda\omega)^2}{1 + (\lambda\omega)^2}, \quad (10)$$

$$\frac{\eta''(\omega)}{\eta_0 - \eta_s} = \frac{3}{5} \frac{\lambda\omega}{1 + (\lambda\omega)^2}. \quad (11)$$

In which the suspension relaxation time is given by [after Eq. (5.1) of Ref. 26]

$$\lambda = \frac{\zeta L^2}{12kT}, \quad (12)$$

where ζ is the friction coefficient, and from which we get the rotational diffusivity [see Eq. (5.1) of Ref. 26; see Footnote 2 of p. 62 of Ref. 15; Eq. (22) of Ref. 14].

$$D_r \equiv \frac{1}{6\lambda}. \quad (13)$$

For Stokes flow around spherical beads

$$\zeta \equiv 3\pi d\eta_s. \quad (14)$$

In commercial vaccine manufacture, mRNA encapsulation can result in at least (i) nanospheres, (ii) planar three-blister structures [top right of Fig. 1 of Ref. 3], (iii) planar four-blister structures [lower left of Fig. 1 of Ref. 3; Fig. 4a (right panel) of Ref. 2], (iv) planar five-blister structures [lower left of Fig. 1 of Ref. 3; Fig. 4a (right panel) of Ref. 2], (v) symmetric nanodumbbells (Fig. 3 of Ref. 5; Fig. 3 of Ref. 2; Fig. 21 of Ref. 33), or (vi) lopsided nanodumbbells (Fig. 3 of Ref. 5; Fig. 3 of Ref. 2; Fig. 21 of Ref. 33). In rigid bead-rod theory, we would call romanette (ii) *center-beaded equilateral triangular* (set $N = 3$ in row 3 of Table XV of Refs 34 and 35), and romanette (iii) *center-beaded square* (set $N = 4$ in row 3 of Table XV of Ref. 34). In mRNA encapsulation, the lopsided nanodumbbell has been called the *predominant morphology*,⁵ and we thus devote this paper to this structure.

Why mRNA encapsulations into lipids take the form of dumbbells is not known. Further, why these dumbbells are lopsided, is also unknown. We do know that the mRNA payloads are anionic, while their encapsulants are cationic. Payload repulsion might therefore be causing the lopsidedness, and if so, the lopsidedness, d_b/d_p , may increase with the number of mRNA strands in the dumbbell bleb. This should be studied.

II. LOSIDED NANODUMBELL GEOMETRY

Whereas the predominant morphology is the lopsided nanodumbbell,⁵ some replace this with nanospheres (*cf.* Fig. 3 with Fig. 2 of Ref. 12), and others, with capsules (*cf.* Fig. 3a with Fig. 3.b of Ref. 5). We can deepen our understanding of the lopsided dumbbell by examining its geometry as intersecting spheres. Its volume is

$$V_\ell = \frac{\pi(d_b + d_p + 2L)^2(3(d_b - d_p)^2 + 4(d_b + d_p)L - 4L^2)}{192L}, \quad (15)$$

in contrast to its symmetric counterpart (of the same length L)

$$V = \frac{\pi}{12}(2d_b - L)(d_b + L)^2, \quad (16)$$

so that

$$\frac{V_\ell}{V} = \frac{\left(\frac{d_p d_b}{L} + \frac{d_p}{L} + 2\right)^2 \left[4 - 4\frac{d_p}{L}\left(\frac{d_b}{d_p} + 1\right) - 3\left(\frac{d_p}{L}\right)^2 \left(\frac{d_b}{d_p} - 1\right)^2\right]}{16\left(1 - 2\frac{d_p d_b}{L}\right)\left(1 + \frac{d_p d_b}{L}\right)^2}, \quad (17)$$

which expands about unit lopsidedness as

$$\frac{V_\ell}{V} = 1 - \frac{3\left(\frac{d_p}{L}\right)^2}{\left(\frac{d_p}{L} + 1\right)\left(2\frac{d_p}{L} - 1\right)}\left(\frac{d_b}{d_p} - 1\right) + \dots \quad (18)$$

or about unit bleb size as

$$\begin{aligned} \frac{V_\ell}{V} = & \frac{\left(3 - 2\frac{d_b}{d_p} + 3\left(\frac{d_b}{d_p}\right)^2\right)\left(9 + 6\frac{d_b}{d_p} + \left(\frac{d_b}{d_p}\right)^2\right)}{16\left(2\frac{d_b}{d_p} - 1\right)\left(1 + \frac{d_b}{d_p}\right)^2} \\ & + \frac{3\left(\frac{d_b}{d_p} - 1\right)\left(\frac{d_b}{d_p} + 3\right)\left(6 + \frac{d_b}{d_p}\left(\left(\frac{d_b}{d_p}\right)^3 - \frac{d_b}{d_p} - 2\right)\right)}{8\left(\frac{d_b}{d_p} + 1\right)^3\left(2\frac{d_b}{d_p} - 1\right)^2} \\ & \times \left(\frac{d_p}{L} - 1\right) + \dots, \end{aligned} \quad (19)$$

from which we learn that the volume of the lopsided dumbbell (relative to its symmetric counterpart) depends upon two ratios: its lopsidedness, d_b/d_p , and its dimensionless bleb size, d_p/L . The volume decreases with both ratios.

The bleb meets the bead devoid of payload at the circle of intersection. We call this the nanodumbbell *waistline*. This waistline touches three phases: (i) the suspending fluid, (ii) the bleb, and (iii) the bead devoid of payload. The waistline diameter is given by

$$d_\ell = \frac{1}{4d_b}\sqrt{16L^2d_b^2 - (4L^2 + d_b^2 - d_p^2)^2}, \quad (20)$$

in contrast to its symmetric counterpart

$$d_i = \sqrt{d_b^2 - L^2}, \quad (21)$$

so that

$$\frac{d_\ell}{d_i} = \frac{1}{4}\sqrt{\frac{16\left(\frac{d_p}{L}\right)^2\left(\frac{d_b}{d_p}\right)^2 - \left(4 + \left(\frac{d_p}{L}\right)^2\left(\frac{d_b}{d_p}\right)^2 - \left(\frac{d_p}{L}\right)^2\right)^2}{\left(\frac{d_p}{L}\right)^2\left(\frac{d_b}{d_p}\right)^2 - 1}}, \quad (22)$$

which expands about unit lopsidedness as

$$\frac{d_\ell}{d_i} = 1 - \frac{\left(\frac{d_p}{L}\right)^2}{2\left(\left(\frac{d_p}{L}\right)^2 - 1\right)}\left(\frac{d_b}{d_p} - 1\right) + \dots \quad (23)$$

or about unit bleb size as

$$\frac{d_\ell}{d_i} = \frac{1}{4} \sqrt{\frac{-9 + 10 \left(\frac{d_b}{d_p}\right)^2 - \left(\frac{d_b}{d_p}\right)^4}{\left(\frac{d_b}{d_p}\right)^2 - 1}} + \frac{\left(6 + 3 \left(\frac{d_b}{d_p}\right)^2 - \left(\frac{d_b}{d_p}\right)^4\right)}{2 \sqrt{\left(-9 + 10 \left(\frac{d_b}{d_p}\right)^2 - \left(\frac{d_b}{d_p}\right)^4\right) \left(\left(\frac{d_b}{d_p}\right)^2 - 1\right)}} \times \left(\frac{d_p}{L} - 1\right) + \dots, \quad (24)$$

from which we learn that the waistline perimeter of the lopsided dumbbell (relative to its symmetric counterpart) depends upon two ratios: its lopsidedness, d_b/d_p , and on its dimensionless bleb size, d_p/L . The waistline diameter increases with both ratios. Figures 4 and 5 show how dimensionless nanodumbbell volume and waistline perimeter descend with dumbbell lopsidedness. The dimensionless bleb size, d_p/L is not to be confused with the particle aspect ratio, $\alpha \equiv d_b/(\frac{1}{2}d_b + \frac{1}{2}d_p + L)$.

The surface area of the nanodumbbell is given by

$$S_\ell = \frac{\pi(4L(d_b^2 + d_p^2) + 4L^2(d_b + d_p) - d_b d_p(d_b + d_p) + (d_b^3 + d_p^3))}{8L}, \quad (25)$$

in contrast to its symmetric counterpart

$$S = \pi d_b(d_b + L), \quad (26)$$

so that

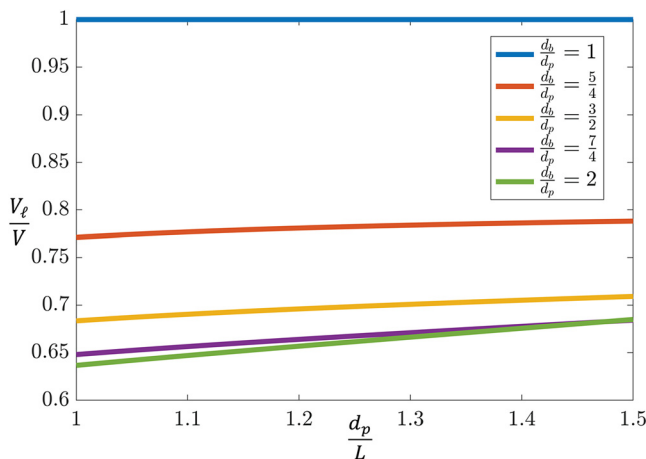


FIG. 4. Descent of dumbbell volume, V_ℓ/V , with dimensionless bleb size, d_p/L , parametrized with lipid nanoparticle lopsidedness, d_b/d_p [Eq. (17)]. $d_b/d_p = [1, \frac{5}{4}, \frac{3}{2}, \frac{7}{4}, 2]$.

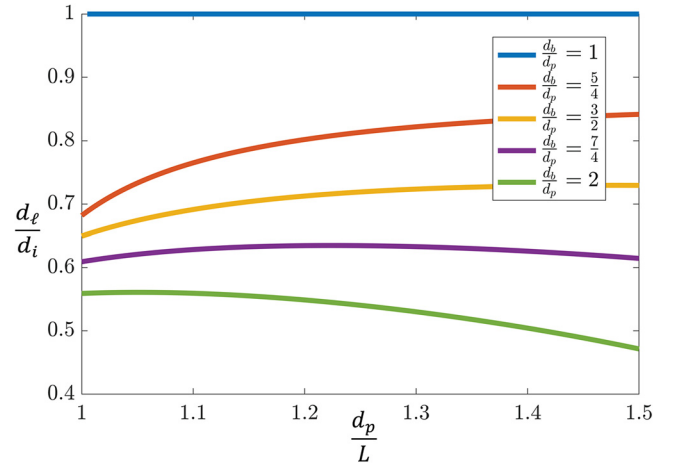


FIG. 5. Descent of waistline perimeter, d_ℓ/d_i , with dimensionless bleb size, d_p/L , parametrized with lipid nanoparticle lopsidedness, d_b/d_p [Eq. (22)]. $d_b/d_p = [1, \frac{5}{4}, \frac{3}{2}, \frac{7}{4}, 2]$.

$$\frac{S_\ell}{S} = \frac{9 + 3 \frac{d_b}{d_p} + 3 \left(\frac{d_b}{d_p}\right)^2 + \left(\frac{d_b}{d_p}\right)^3}{8 \frac{d_b}{d_p} \left(1 + \frac{d_b}{d_p}\right)} + \frac{\left(6 - 5 \frac{d_b}{d_p} - 3 \left(\frac{d_b}{d_p}\right)^2 + \left(\frac{d_b}{d_p}\right)^3 + \left(\frac{d_b}{d_p}\right)^4\right)}{8 \frac{d_b}{d_p} \left(1 + \frac{d_b}{d_p}\right)^2} \left(\frac{d_p}{L} - 1\right) + \dots, \quad (27)$$

which expands about unit bleb size as

$$\frac{S_\ell}{S} = 1 + \frac{1}{2} \left(1 - \frac{d_b}{d_p}\right) + \frac{1}{4} \left(2 + \left(\frac{d_p}{L}\right)^2\right) \left(-1 + \frac{d_b}{d_p}\right)^2, \quad (28)$$

which expands about unit lopsidedness as

$$\frac{S_\ell}{S} = 1 + \frac{\left(-1 - 2 \frac{d_p}{L}\right)}{2 \left(1 + \frac{d_p}{L}\right)} \left(\frac{d_b}{d_p} - 1\right) + \dots. \quad (29)$$

Figure 6 shows the gentle ascents of the dimensionless nanodumbbell surface areas with the dimensionless bleb size, parametrized with dumbbell lopsidedness. In addition, the dimensionless nanodumbbell surface areas descend with dumbbell lopsidedness. Table III uses Eqs. (3)–(5) to arrive at the median geometric properties of the mRNA LNP nanodumbbell. For reference, by volume, the mRNA LNP nanodumbbell is about one thousand times smaller than a red blood cell. A median width mRNA lipid nanoparticle (LNP) nanodumbbell is approximately 1500 times thinner than a human hair and about 25

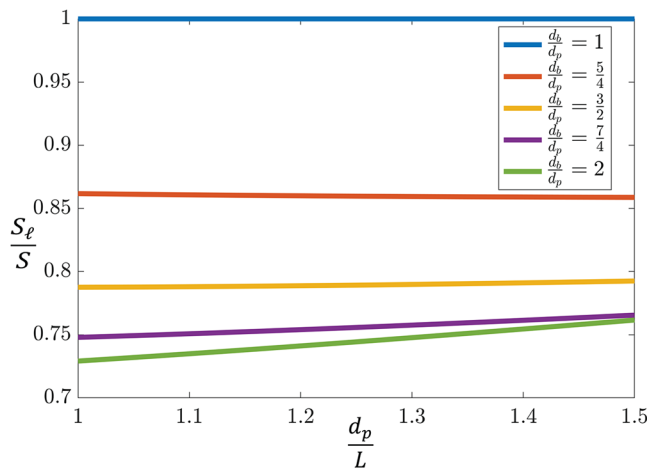


FIG. 6. Descent of surface area, S_ℓ/S , with dimensionless bleb size, d_p/L , parametrized with lipid nanoparticle lopsidedness, d_b/d_p [Eq. (28)]. $d_b/d_p = [1, \frac{5}{4}, \frac{3}{2}, \frac{7}{4}, 2]$.

TABLE III. Lopsided nanodumbbell geometry.

Property	Equation	Median
L	(3)	36 nm
d_p	(4)	37 nm
d_b	(5)	51 nm
d_ℓ	(20)	18 nm
V_ℓ	(15)	$9.40 \times 10^4 \text{ nm}^3$
S_ℓ	(25)	$1.14 \times 10^4 \text{ nm}^2$

times as wide as a doubly helical strand of DNA. The median mRNA nanodumbbell is about 50% longer than it is wide.

III. LOPSIDED RIGID DUMBBELL MODEL

Long before mRNA was encapsulated into lipid nanoparticles, driven purely by curiosity, Abdel-Khalik and Bird undertook the study of lopsided dumbbell suspensions.⁶ Since a lopsided dumbbell consists of two different (rigidly separated) beads, we associate with it two friction coefficients: one for the payloaded bead, ζ_p , and another for the other larger bead, ζ_b . The friction coefficient of a symmetric rigid dumbbell in suspension has been related to those of the lopsided dumbbell [between Eqs. (7) and (8) of Ref. 6; Footnote 3 on p. 522 and Table XIII.IV-I of Ref. 13; cf. Eq. (10.6-1) of Ref. 13; Table XVI.IV-I of Ref. 15]:

$$\frac{2}{\zeta} = \frac{1}{\zeta_p} + \frac{1}{\zeta_b}, \quad (30)$$

wherein, following Eq. (14), $\zeta_p \equiv 3\pi d_p \eta_s$ and $\zeta_b \equiv 3\pi d_b \eta_s$. Reference 6 thus teaches that [Eq. (11) of Ref. 6]: “all results ... for symmetrical dumbbells can be taken over for lopsided dumbbells simply by replacing $2/\zeta$ everywhere by $(1/\zeta_p + 1/\zeta_b)$.”

For instance, from Eq. (12), for our lipid nanodumbbells, we get

$$\lambda_\ell = \left(\frac{1}{\zeta_p} + \frac{1}{\zeta_b} \right)^{-1} \frac{L^2}{6kT}, \quad (31)$$

where L is still the center-to-center distance between the beads. Hence

$$\lambda_\ell = \left(\frac{1}{d_p} + \frac{1}{d_b} \right)^{-1} \frac{\pi \eta_s L^2}{2kT} \quad (32)$$

from which we learn that the relaxation time of the lopsided liquid nanoparticle increases with the square of its center-to-center length, L . With Eqs. (12) and (14), Eq. (32) non-dimensionalizes to

$$\frac{\lambda_\ell}{\lambda} = \frac{2 \left(\frac{1}{d_p} + \frac{1}{d_b} \right)^{-1}}{d}. \quad (33)$$

We next compare the relaxation time of the lopsided dumbbell with its symmetric counterpart of bead diameter d_b ,

$$\frac{\lambda_\ell}{\lambda} = 2 \left(\frac{d_b}{d_p} + 1 \right)^{-1}, \quad (34)$$

which we illustrate in Fig. 7, from which we learn that the relaxation time of the mRNA encapsulated dumbbell descends with its aspect ratio, d_b/d_p . The larger the mRNA payloaded bead, d_p , the lower the relaxation time, λ_ℓ .

Equation (34) does not contain the bead masses, m_b and m_p . This might strike the uninitiated as odd. However, the masses of the lopsided dumbbells of Ref. 6 cancel. In other words, the added mass of the mRNA payload plays no role in the transport properties of the mRNA payloaded nanodumbbells.

From the rheological material functions in Eqs. (7)–(11), for mRNA encapsulating nanodumbbells, the dumbbell contribution to the zero-shear viscosity is

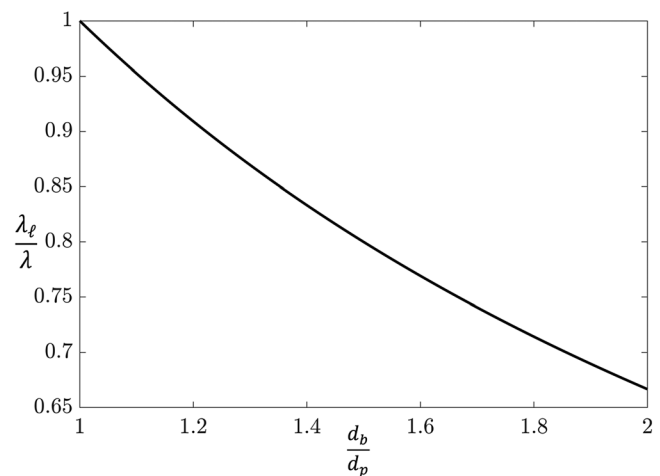


FIG. 7. Descent of dimensionless relaxation time, λ_ℓ/λ , with lipid nanoparticle lopsidedness, d_b/d_p [Eq. (34)]. $d_b/d_p = [1, \frac{5}{4}, \frac{3}{2}, \frac{7}{4}, 2]$ (encapsulated mRNA is closest to $d_b/d_p = 2$). Since $\eta_0 - \eta_s$ is proportional to relaxation time [Eqs. (7) or (35)], the polymer contribution to the zero-shear viscosity will descend identically with lopsidedness.

$$\eta_0 - \eta_s = nkT\lambda_\ell, \quad (35)$$

the steady shear viscosity is

$$\frac{\eta(\dot{\gamma}) - \eta_s}{\eta_0 - \eta_s} = 1 - \frac{18}{35}(\lambda_\ell \dot{\gamma})^2 + \frac{1326}{1925}(\lambda_\ell \dot{\gamma})^4 + \dots \quad (36)$$

The shear stress relaxation following step shear is

$$G(t) = \left(2\eta_s + \frac{4}{5}nkT\lambda_\ell \delta(t)\right) + \frac{3}{5}nkTe^{-t/\lambda_\ell}, \quad (37)$$

and the viscous and *minus* the elastic parts of the complex viscosity are given as

$$\frac{\eta'(\omega) - \eta_s}{\eta_0 - \eta_s} = 1 - \frac{3}{5} \frac{(\lambda_\ell \omega)^2}{1 + (\lambda_\ell \omega)^2}, \quad (38)$$

$$\frac{\eta''(\omega)}{\eta_0 - \eta_s} = \frac{3}{5} \frac{\lambda_\ell \omega}{1 + 4(\lambda_\ell \omega)^2}, \quad (39)$$

where λ_ℓ is given by Eq. (34), $\lambda_\ell \dot{\gamma}$ is called the Weissenberg number, and $\lambda_\ell \omega$, the Deborah number. The material functions of Eqs. (35)–(38) are interrelated by

$$\eta_0 = \lim_{\dot{\gamma} \rightarrow 0} \eta(\dot{\gamma}) = \int_0^\infty G(t)dt = \lim_{\omega \rightarrow 0} \eta'(\omega). \quad (40)$$

Both $\lambda_\ell \dot{\gamma}$ and $\lambda_\ell \omega$ are properties of both the mRNA-loaded suspensions, and of the laboratory homogeneous flow fields used to measure said properties. Whereas $\lambda_\ell \dot{\gamma}$ governs the nonlinearity of the fluid and the flow, $\lambda_\ell \omega$ governs their elasticity. Equation (38) expands as

$$\frac{\eta'(\omega) - \eta_s}{\eta_0 - \eta_s} = 1 - \frac{3}{5} [(\lambda_\ell \omega)^2 - (\lambda_\ell \omega)^4 + \dots], \quad (41)$$

which we will use below. Also, from Eq. (13) we get the rotational diffusivity of the lopsided rigid nanodumbbell in suspension as

$$D_{r\ell} \equiv \frac{1}{6\lambda_\ell}. \quad (42)$$

In this work, we focus on just four important rheological material functions. However, our method applies equally to any material functions known for symmetric rigid dumbbells.²⁶

IV. HOOKEAN ELASTIC DUMBBELL MODEL

For symmetric Hookean dumbbells the viscous and *minus* the elastic parts of the complex viscosity are given by [Eqs. (13.4–21) and (13.4–22) of Ref. 15]

$$\frac{\eta'(\omega) - \eta_s}{\eta_0 - \eta_s} = \frac{1}{1 + (\lambda_H \omega)^2}, \quad (43)$$

$$\frac{\eta''(\omega)}{\eta_0 - \eta_s} = \frac{\lambda_H \omega}{1 + (\lambda_H \omega)^2}, \quad (44)$$

in which (see Eq. (13.4–4) of Ref. 15]

$$\lambda \equiv \frac{\zeta}{4H}, \quad (45)$$

where H is the spring stiffness (and thus, in the present context the nanodumbbell stiffness). For lopsided Hookean dumbbells, recent

theory suggests that the relaxation time, λ_H , can be replaced with [Eq. (25) of Ref. 7]

$$\frac{\lambda_{H\ell}}{\lambda_H} = 2 \left(\frac{d_b}{d_p} + 1 \right)^{-1}, \quad (46)$$

so that Eqs. (43) and (44) become

$$\frac{\eta'(\omega) - \eta_s}{\eta_0 - \eta_s} = \frac{1}{1 + (\lambda_{H\ell} \omega)^2}, \quad (47)$$

$$\frac{\eta''(\omega)}{\eta_0 - \eta_s} = \frac{\lambda_{H\ell} \omega}{1 + (\lambda_{H\ell} \omega)^2}, \quad (48)$$

wherein Eq. (47) expands as

$$\frac{\eta'(\omega) - \eta_s}{\eta_0 - \eta_s} = 1 - (\lambda_{H\ell} \omega)^2 + (\lambda_{H\ell} \omega)^4 - \dots \quad (49)$$

By comparing the leading coefficient with Eq. (41), we get

$$\frac{\lambda_{H\ell}}{\lambda_\ell} = \sqrt{\frac{3}{5}}, \quad (50)$$

which we will use as a consistency check below, and which with Eqs. (45) and (12), implies that

$$\frac{HL^2}{kT} = \sqrt{15}. \quad (51)$$

Also, from Eq. (13) we get the rotational diffusivity of the Hookean elastic nanodumbbell in suspension

$$D_{H\ell} \equiv \frac{1}{6\lambda_{H\ell}}, \quad (52)$$

which we will use below. Combining Eq. (52) with Eq. (42) gives

$$\frac{D_{rH\ell}}{D_{r\ell}} = \frac{\lambda_\ell}{\lambda_{H\ell}} = \sqrt{\frac{5}{3}} \quad (53)$$

which we believe to be new.

V. RESULTS AND DISCUSSION

From Figs. 8 and 9, we observe that dumbbell lopsidedness shifts the dimensionless steady shear viscosity and the viscous part of the complex viscosity curves to the right. In other words, nanodumbbell lopsidedness increases the dimensionless viscosity of the nanodumbbell suspensions. Fitting Eq. (36) with Eq. (34) to steady shear viscosity measurements enables determination of the viscosity average lopsidedness, d_b/d_p of the nanodumbbell suspension. Similarly, by fitting Eq. (38) with Eq. (34) to the real part of the complex viscosity enables determination of the viscosity average lopsidedness, d_b/d_p , of the nanodumbbell suspension. Though our work is motivated mainly by curiosity, herein lies the usefulness of our main results.

From Fig. 10 we learn that the dumbbell lopsidedness shifts *minus* the dimensionless elastic part of the complex viscosity curves to the right. Otherwise put, nanodumbbell lopsidedness increases the elasticity of the nanodumbbell suspensions.

As consistency checks, we can report that (i) the $d_b/d_p = 1$ curve of Fig. 8 for the symmetric dumbbell agrees with Fig. 3a. of Ref. 26, as it should, that (ii) the $d_b/d_p = 1$ curve of Fig. 9 agrees with the $h = 0$

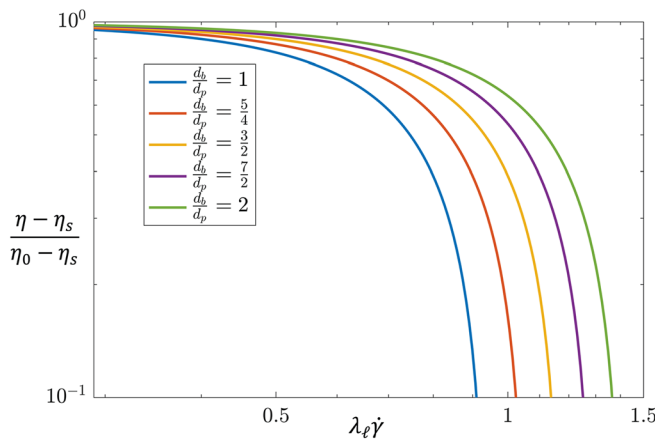


FIG. 8. Effect of lipid nanoparticle lopsidedness d_b/d_p on steady shear viscosity [Eq. (36) with Eq. (34)]. $d_b/d_p = [1, \frac{5}{4}, \frac{3}{2}, \frac{7}{4}, 2]$.

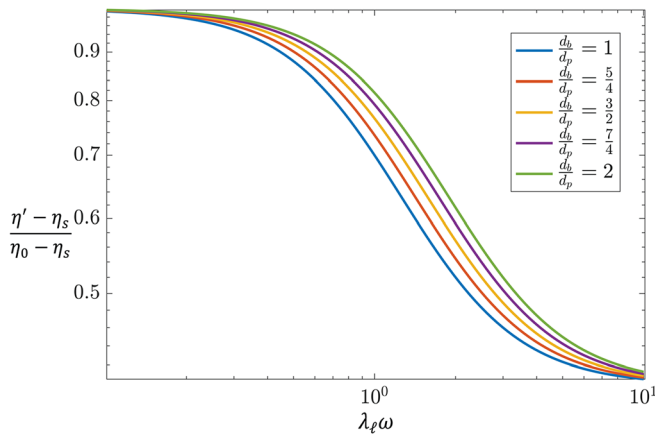


FIG. 9. Effect of lipid nanoparticle lopsidedness d_b/d_p on the real (viscous) part of the complex viscosity [Eq. (38) with Eq. (34)]. $d_b/d_p = [1, \frac{5}{4}, \frac{3}{2}, \frac{7}{4}, 2]$.

curve of Fig. 3f of Ref. 26, as it should, that (iii) the $d_b/d_p = 1$ curves of Figs. 9 and 10 agree with the corresponding $2b/av = 3/2$ curves of Fig. 4 of Ref. 34, as they should, and that (iv) the $d_b/d_p = 1$ curve of Fig. 8 for the symmetric dumbbell agrees with the $I_3/I_1 = 0$ curve of Fig. 1 of Ref. 36, as it should.

VI. WORKED EXAMPLE: RIGID VS ELASTIC

We next test our competing theories against experimental observations of vaccine nanodumbbell contribution of HA-mRLNPs to hyaluronan suspension. For this, we rely upon measurements from Fig. S11. of Ref. 37 showing the rheological behaviors of HA-mRLNPs to hyaluronan suspension. Specifically, we will compare the viscous part (η') and *minus* the elastic part (η'') of the complex viscosity with both lopsided rigid dumbbell theory [Sec. III; Eqs. (38) and (39)] and Hookean elastic dumbbell theory [Sec. IV; Eqs. (47) and (48)] to evaluate their accuracies for the viscoelastic behaviors of mRNA LNP suspensions. By hyaluronan (polyhyaluronic acid) we mean the linear

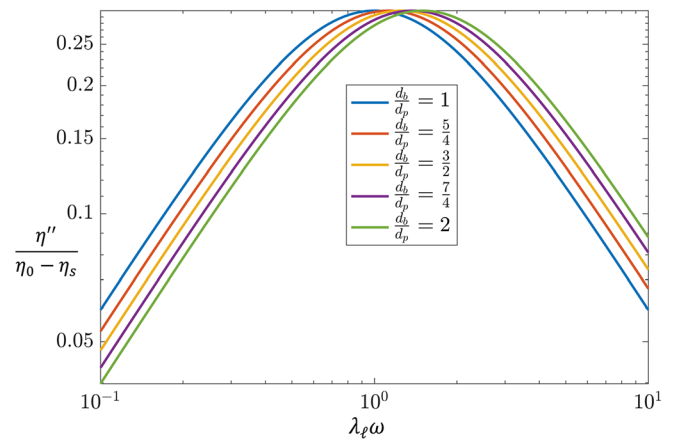


FIG. 10. Effect of lipid nanoparticle lopsidedness d_b/d_p on *minus* the imaginary (elastic) part of the complex viscosity [Eq. (39) with Eq. (34)]. $d_b/d_p = [1, \frac{5}{4}, \frac{3}{2}, \frac{7}{4}, 2]$.

high-molecular weight polysaccharide found in the extracellular matrix, especially of soft connective tissues.³⁸

From Fig. 11(a), we glean the best fit values $\eta_0 = 3.8$ Pa s and $\lambda_\ell = 0.057$ s. From Fig. 11(a), we learn that $\eta'(\omega)$ from lopsided rigid dumbbell theory is well behaved at low frequency ($\lambda_\ell \omega \leq 1$) but otherwise, overpredicts. Further, Fig. 11(b) shows that the lopsided rigid dumbbell theory underpredicts $\lambda_\ell \omega$ for all frequencies, though it does get the peak frequency, $\lambda_\ell \omega_p \cong 1$, about right. Recall that Fig. 11(b) relies upon the same best-fit values of η_0 and λ_ℓ from $\eta'(\omega)$ of Fig. 11(a). From Eq. (42), we calculate the rotational diffusivity for lopsided rigid nanodumbbells in suspension as $D_{r\ell} = 2.92$ s⁻¹. This calculation, however, neglects the deformability of the mRNA loaded LNP nanodumbbell. The failures of the rigid theory to explain the behavior of the mRNA contributions to the complex viscosity motivated our use of the elastic dumbbell theory.

From Fig. 12(a), we glean the best fit values $\eta_0 = 3.8$ Pa s and $\lambda_{H\ell} = 0.044$ s. The fitted values $\lambda_{H\ell} = 0.044$ s and $\lambda_\ell = 0.057$ s satisfy the self-consistency relation Eq. (50), as they must. By contrast with lopsided rigid dumbbell theory, from Fig. 12(a) we learn that $\eta'(\omega)$ from Hookean elastic dumbbell theory is well behaved at all frequencies. Further, Fig. 12(b) shows Hookean elastic dumbbell theory to be far more accurate than lopsided rigid dumbbell theory [compare with Fig. 11(b)]. Recall that Fig. 12(b) relies upon the same best fit values of η_0 and $\lambda_{H\ell}$ from $\eta'(\omega)$ of Fig. 12(a). It would appear that the nanodumbbells of mRNA loaded LNP suspensions, even in the gentlest of flows (small-amplitude oscillatory shear flow), deform. From Eq. (52) we calculate the rotational diffusivity for Hookean elastic nanodumbbells in suspension and we get $D_{rH\ell} = 3.78$ s⁻¹, which is higher than the value $D_{r\ell} = 2.92$ s⁻¹ obtained above by neglecting the deformability of the mRNA-loaded LNP nanodumbbell.

Solving Eq. (51) gives

$$H = \sqrt{15} \frac{kT}{L^2}, \quad (54)$$

which, combined with Eq. (3), gives

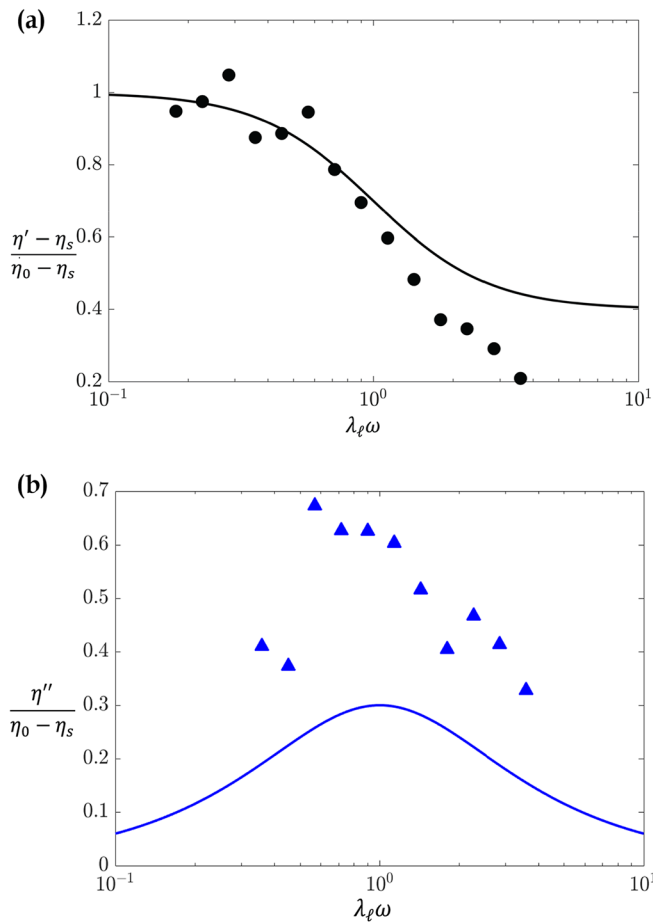


FIG. 11. Measured vaccine nanodumbbell contribution of HA-mRLNPs to hyaluronan suspension vs lopsided rigid dumbbell theory from (a) Eq. (38) for real part of complex viscosity (black circles vs solid black curve) and (b) Eq. (39) for *minus* the imaginary part (blue triangles vs solid blue curve) ($\eta_0 = 3.8$ Pa s, $\lambda_\ell = 0.057$ s, $c = 32$ mg/ml).

$$9 \lesssim H \lesssim 19 \mu\text{N/m}, \quad (55)$$

for the deforming nanodumbbell stiffness range. This is a main result of this work. From Eq. (55), we can assign an effective axial Young's modulus

$$E = \frac{4HL}{\pi d_\ell^2} = \frac{60}{\sqrt{15}} \frac{kT}{\pi d_\ell^2 L}. \quad (56)$$

Which, using Table III, gives the median effective axial Young's modulus as

$$E = \frac{4HL}{\pi d_\ell^2} = 2 \text{ kPa} \quad (57)$$

of the mRNA nanodumbbell encapsulate. Though the local superficial elastic modulus can be measured by nano indentation using an atomic force microscope, we know of no one having reported such measurements (see Fig. 5 of and absence from Ref. 39). Our rheological

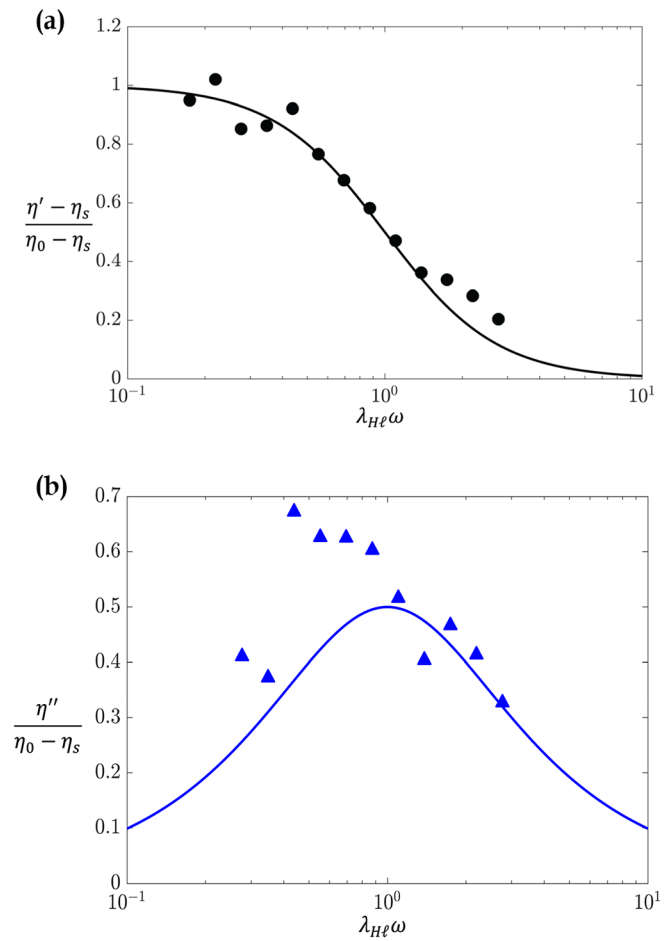


FIG. 12. Measured vaccine nanodumbbell contribution of HA-mRLNPs to hyaluronan suspension vs Hookean elastic dumbbell theory from (a) Eq. (47) for real part of complex viscosity (black circles vs solid black curve) and (b) Eq. (48) for *minus* the imaginary part (blue triangles vs solid blue curve) ($\eta_0 = 3.8$ Pa s, $\lambda_{H\ell} = 0.044$, $c = 32$ mg/ml).

determination of the modulus 2 kPa for the mRNA LNP is nonlocal, axial, for the whole particle. We know of no comparable measurement. In addition, as a practical reference, following linear elastic indentation mechanics, an elastic medium with $E = 2$ kPa would register a durometer reading of just 0.035 on Scale DO standardized in ASTM D2240.^{40–42} The durometer needle would thus hardly deflect. The mRNA nanodumbbells are indeed soft matter.

VII. CONCLUSION

We have deepened our understanding of the predominant morphology of a suspension of mRNA encapsulated into lipid nanoparticles, namely the suspension of lopsided dumbbells. By *lopsided*, we mean that the payloaded bead is smaller than the bead without payload. We arrive at analytical expressions for the four most important rheological material functions.

Our main results, Eqs. (35)–(39), suggest a means of measuring λ_ℓ from rheological characterizations of mRNA-payloaded lipid

nanodumbbell suspensions. Moreover, using Fig. 8 or Fig. 9, the viscosity average lopsidedness, \bar{d}_b/d_p , can be deduced from the shapes of the measured $\eta(\dot{\gamma})$ or $\eta'(\omega)$ curves respectively. From Eq. (13) for lopsided nanodumbbells, we recall that

$$D_{r\ell} \equiv \frac{1}{6\lambda_\ell}. \quad (42)$$

To our knowledge, the rotational diffusivities of mRNA-payloaded lipid nanodumbbell suspensions have not been measured. Moreover, the rotational diffusivities of model lopsided dumbbell suspensions have not been measured. By contrast, rotational diffusivity measurements of symmetric polymer dumbbells in suspension have been measured.⁴³ Taking into account for the deformability of the mRNA-loaded nanodumbbell encapsulates, from the small-amplitude oscillatory shear measurements, we arrive at the rotational diffusivity of $D_{rH\ell} = 3.78 \text{ s}^{-1}$.

Rigid dumbbells cannot deform. By this we mean, that they cannot lengthen, shorten, twist, or bend. We find poor agreement for *minus* the elastic part of the complex viscosity, and better agreement for the viscous part, between measured mRNA lipid nanodumbbell behaviors and rigid dumbbell theory in small-amplitude oscillatory shear flow (Fig. 11). This suggests that mRNA lipid nanodumbbells are (α) deforming in small-amplitude oscillatory shear flow, and (β) that these deformations matter.

Recall that Hookean dumbbells can lengthen and shorten but cannot twist or bend. We find good agreements, for both the viscous part and *minus* the elastic part of the complex viscosity, between measured mRNA lipid nanodumbbell behaviors and lopsided Hookean dumbbell theory in small-amplitude oscillatory shear flow (Fig. 12). These good agreements suggest that mRNA lipid nanodumbbells are lengthening or shortening in small-amplitude oscillatory shear flow. These good agreements also suggest that mRNA lipid nanodumbbells are (a) neither twisting nor bending, or (b) that their twisting and bending contributes negligibly to their complex viscosity.

Our work here focuses on the *predominant morphology*⁵ of an mRNA encapsulation by lipid, the nanodumbbell. However, other intriguing shapes are observed, including the center-beaded equilateral triangular, center-beaded square, and center-beaded pentagonal mRNA encapsulations of Figs. 13, 14, and 15, respectively. Whether such multi-bleb configurations are advantageous for vaccination or not is unclear. Is the mRNA of the secondary, tertiary, quarternary or quinary encapsulations wasted? Otherwise put, can more than one mRNA from a multi-bleb encapsulation vaccinate, or are these extra blebs wasting product?

We find the mRNA encapsulations of Figs. 13–15 to be intrinsically beautiful. To arrive at analytical expressions for the transport properties of suspensions of these oblate mRNA encapsulations of Figs. 13–15, we would use rotarance theory. Specifically, for the former we would start with the planar 3-arm star (setting $N = 3$ in row 3 of Table XV of Ref. 34), and for the latter, the planar 4-arm star (setting $N = 4$ in row 3 of Table XV of Ref. 34). Allowing for the bleb masses and diameters to differ from the central larger bead devoid of payload would follow.⁶ We leave this intriguing task for another day.

Our work on lopsided dumbbell lipid nanoparticles is silent on intraparticle hydrodynamic interaction,^{44–47} that is, on the interferences of the Stokes flow velocity profiles between the two spheres (of different diameter) (see above Eq. (10.6–1) of Ref. 13). For rigid

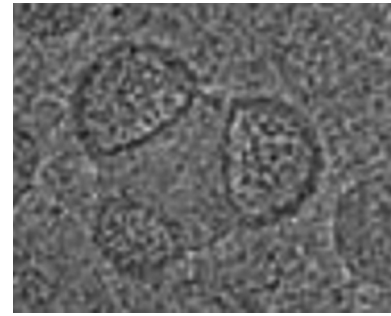


FIG. 13. Center-beaded equilateral triangular mRNA encapsulation into lipid nanoparticle. Reproduced with permission from Brader *et al.*, *Biophys. J.* **120**, 2766–2770 (2021). Copyright 2021 Elsevier (Cell Press) (Supplementary Data S2 of Ref. 2).



FIG. 14. Center-beaded square mRNA encapsulation into lipid nanoparticle. Reproduced with permission from Brader *et al.*, *Biophys. J.* **120**, 2766–2770 (2021). Copyright 2021 Elsevier (Cell Press) (Fig. 4a (right panel) of Ref. 2).



FIG. 15. Center-beaded pentagonal mRNA encapsulation into lipid nanoparticle. Reproduced with permission from Brader *et al.*, *Biophys. J.* **120**, 2766–2770 (2021). Copyright 2021 Elsevier (Cell Press) (Fig. 4a (right panel) of Ref. 2).

dumbbells, when the two spheres do not differ, the effects of hydrodynamic interactions are well-known [Eqs. (42) of Ref. 48]. By contrast, for lopsided Hookean elastic dumbbells such as mRNA-payloaded lipid nanodumbbells, the Stokes flow interferences between unlike beads have not been worked out (see § 13.6 of Ref. 15). We leave this important exploration for another day.

Our work on lopsided dumbbell lipid nanoparticles addresses the deformability of the nanodumbbells during flow. The beads of Figs. 2 or 3 are not, after all, rigidly separated and rigidly positioned relative to one another. With the Hookean elastic dumbbell, we allow the lopsided dumbbell to extend or compress, but do not allow it to twist or bend.⁴⁹ We leave the exploration of the twisting and bending of these intriguing nanodumbbells for another day.

Our work here focused on the complex viscosity, to the exclusion of other rheological material functions. For the Hookean dumbbell suspension, we get a constitutive equation of the form of the upper-convected Jeffreys model, also called Oldroyd-B (see § 13.4. of Ref. 15). The mRNA nanodumbbell contributions to other rheological material functions can thus be predicted, more or less realistically, from this constitutive theory (see § 24. of Ref. 26).

Since both rigid and elastic dumbbell models are equally accurate for $\eta'(\omega)$ at low frequency, we arrive at two bridging relations between the dumbbell models, Eqs. (50), (51), and (53), which we believe to be new. We used Eq. (51) to arrive at the median value of the spring constant for the mRNA nanodumbbell encapsulates of $H = 14 \mu\text{N/m}$. We further assign an effective axial Young's modulus to the mRNA nanodumbbell encapsulates of $E = 2 \text{ kPa}$.

Our work is also silent on any difference in charge between the dumbbell beads. To our knowledge, the charge distribution over the payloaded nanodumbbells has not been measured. The payloaded blebs might be expected to be locally anionic, and the larger bead, devoid of payload, cationic. How dipolar symmetric rigid dumbbells orient under a constant electrical field in steady shear flow is well understood.⁵⁰ How this constant electrical field affects the steady shear material functions for dipolar symmetric rigid dumbbell is also well understood.⁵⁰ The viscosity average dipole of the payloaded nanodumbbell suspensions might thus be deduced from the steady shear rheology of the suspension.

Symmetric rigid dumbbells in suspension will migrate toward walls in heterogeneous pressure-driven flow fields.⁵¹ In microfluidic applications, we thus expect the payloaded nanodumbbells to concentrate away from the walls of a shear flow.⁵² The analytical solutions for symmetric dumbbell migration of Ref. 51 can thus be taken over, for lopsided nanodumbbells, by the method of Ref. 6. Near walls, dumbbell suspensions are also known to orient in the plane of the wall, and that this orientation will persist for some distance from that wall. In parallel disk rheometry, this is observed as gap dependence at small gaps.^{53–56} Specifically, both $\eta'(\omega)$ and $\eta''(\omega)$ are observed to decrease with symmetric dumbbell confinement. For lopsided rigid dumbbells, analytical solutions for this can be adopted following Ref. 6.

Though our work has focuses on payloaded lipid nanoparticles, other biological suspensions of lopsided dumbbells have not escaped our attention. For instance, lopsided dumbbell suspensions arise when certain viral proteins interact with membranes (see Figs. 1–3 of Ref. 57). Further, lopsided microdumbbell suspensions (of uniform size and lopsidedness) of polymethylmethacrylate⁵⁸ or of polystyrene⁵⁹ have been synthesized. Symmetric dumbbells consisting of one polystyrene bead and the other polymethylmethacrylate have also been synthesized, and their rotational diffusivity has also been measured optically.⁴³ These intriguing particles would serve as ideal model lopsided dumbbells, to test any of the main results of this work [Eqs. (35)–(39)] in the laboratory. However, we know of no rheological characterizations of such lopsided dumbbell suspensions.

In this work, we have focused on just one material function, the mildest, small-amplitude oscillatory shear flow. However, our discovery that Hookean dumbbell theory predicts the behaviors of lopsided mRNA-loaded LNP suspensions suggests that we might be able to extend our prediction to other material functions using the tensor-valued constitutive equation for Hookean dumbbells: the convected Jeffreys model [Eqs. (13.4–5) and (13.4–9) of Ref. 15].

We are aware that the encapsulating surface and the mRNA payload have different charge (Fig. 1 of Ref. 9). Further, the empty and loaded blebs may have different charge. Our work here is silent on such electrostatic lopsidedness. To account for this, we would start from scratch by incorporating the contribution of the external force term in Eq. (13.3–14) of Ref. 15. We leave this daunting exploration for another day.

From atomic force microscopy, we can extract micromechanical properties of nanoparticles, including their indentation hardness. Much has been written about this for lipid nanoparticles,^{60–63} including those encapsulating mRNA.³⁹ If the particle structure is known, and the linear elastic indentation mechanics of said structure are also known, Young's moduli or thicknesses can be deduced from the lipid shell stiffnesses (see the only equation in Ref. 64)

$$k_i = \frac{8E_i h_i^2}{d_i \sqrt{3(1-\nu^2)}}, \quad (58)$$

where $i \equiv p$ means payloaded bleb and $i \equiv b$ means empty bead. We use the symbol k_i here because Ref. 64 does not report if the atomic force micromechanical measurement of its Fig. 5(a) is performed on a bleb or on an empty bead. Whereas the linear elastic indentation mechanics of a spherical shell are known (Eq. (49) of Ref. 65), to our knowledge, the linear elastic indentation mechanics of a nanodumbbell shell are unknown. Otherwise put, the linear elastic indentation mechanics along the axis of a lopsided nanodumbbell have yet to be worked out. We leave the micromechanics of this predominant nanodumbbell morphology of mRNA encapsulates, for another day.

When a hemispherical tip indents a thick linear elastic solid, it produces nonlinear load vs penetration of infinite initial slope [see Eq. (8) of Ref. 41]. When a hemispherical tip indents a linear elastic shell, proportional load vs penetration obtains (see the only equation in Ref. 64). When the hemispherical tip of an atomic force microscope indents lipid nanoparticles, proportional load vs penetration results (see Fig. 3 of Ref. 64). This includes lipid layers encapsulating mRNA into vaccines, including the skins of nanodumbbells (see Fig. 5a of Ref. 39 mindful of Region (b) of Fig. 3 of Ref. 39). The mRNA is thus encapsulated by linear elastic lipid shells.

Equation (58) interrelates the properties of the lipid shells. These are not to be confused with properties of the whole nanodumbbell. Still, we can compare analogous quantities: lipid skin stiffness (k) vs axial nanodumbbell stiffness (H). From Fig. 5a of Ref. 39, for the lipid shell stiffnesses, $k_i \cong 33.5 \text{ mN/m}$. Recall, from the complex viscosity, we get the median value $H \cong 14 \mu\text{N/m}$ from Eq. (55). We thus find that indenting the skin of the nanodumbbell is about 10^3 times harder than stretching or compressing it axially. By *harder*, we mean requiring more work for the same displacement.

Solving Eq. (58)

$$h_i^2 E_i = \frac{k_i d_i \sqrt{3(1-\nu^2)}}{8}, \quad (59)$$

from which we get the median values for these products of $h_p^2 E_p \cong 0.23$ nN and $h_b^2 E_b \cong 0.18$ nN (for $k_p \cong k_b \cong k_i$). Were the thicknesses of the lipid nanoparticle shells known, we could deduce the moduli of these shells. To our knowledge, for mRNA encapsulates, these thicknesses are not known.

We have learned that by fitting Eq. (38) with Eq. (34) to the real part of the complex viscosity, we can determine the viscosity average lopsidedness, $\overline{d_b/d_p}$, of the nanodumbbell suspension. The usefulness of our work extends beyond understanding the structure of vaccines through their rheology. Specifically, the mixing of the fragile mRNA lipid nanoparticles during manufacture benefits directly from our findings. Mixing is critical in ensuring uniform size and encapsulation efficiency of LNPs, as it strongly influences nanoparticle self-assembly at the nanoscale. By incorporating dimensionless groups that include the transport properties explored herein (such as viscosity, diffusivities, and flow lopsidedness), our method guides the design and optimization of mixing conditions. This has direct applications in scaling up mRNA vaccine manufacture, where maintaining LNP quality consistently across different production scales is a major challenge. Understanding the rheological behavior of the precursor solutions, informed by our work, allows for better prediction and control of the flow and mixing regimes that are crucial for efficient and reproducible vaccine formulation.^{66–68}

In vaccine mass production, the throughput is limited by lopsided nanoparticle fragility. Our work on elastic dumbbells opens the door to understanding this fragility more deeply. Which mole fraction of the nanodumbbells break might just be which fraction of the elastic dumbbells extended beyond some critical extension. The configuration distribution of the nanodumbbells after all, contains the distribution of their extensions. We leave the intriguing pursuit of the mole fraction of broken nanodumbbells for another day.

Herein, the intriguing work on lopsided dumbbells, undertaken 50 years ago by Abdel-Khalik and Bird,⁶ driven by curiosity, found usefulness in deepening our understanding of mRNA vaccine manufacture.

That the production of mRNA vaccine was accomplished under pandemic pressures has not escaped our attention. Our work on the transport properties of this intriguing vaccine has deepened our appreciation for the engineers and scientists who brought this product urgently to market. We regard the lipid encapsulation of mRNA vaccine not only as intrinsically beautiful, but as one of the finer things of which mankind is capable. Those who created this lifesaving product gave our scientific community its finest hour. We close on this cheerful historical note.

ACKNOWLEDGMENTS

This research was supported by the U.S. Food and Drug Administration under the FDA BAA-22-00123 program (Award No. 75F40122C00200). We thank Professor Nhan Phan-Thien of the National University of Singapore for helpful discussions. We thank the organization of the Division of Fluid Dynamics in the *American Physical Society* in Salt Lake City, Utah held over November 24–26, 2024 for creating the platform at which, and for bringing together the audience to which, this work was first presented.

AUTHOR DECLARATIONS

Conflict of Interest

The authors have no conflicts to disclose.

Author Contributions

M. A. Kanso: Investigation (equal); Methodology (equal); Software (equal); Validation (equal); Visualization (equal); Writing – original draft (equal). **S. Singh:** Conceptualization (equal); Resources (equal). **A. J. Giacomini:** Validation (equal); Writing – review & editing (equal). **Richard D. Braatz:** Supervision (equal); Writing – review & editing (equal).

DATA AVAILABILITY

The data that support the findings of this study are available within the article.

REFERENCES

- ¹B. Jens, “A perspective on bleb and empty LNP structures,” *J. Controlled Release* **373**, 952–961 (2024).
- ²M. L. Brader, S. J. Williams, J. M. Banks, W. H. Hui, Z. H. Zhou, and L. Jin, “Encapsulation state of messenger RNA inside lipid nanoparticles,” *Biophys. J.* **120**, 2766–2770 (2021).
- ³L. Jin, C. W. Jarand, M. L. Brader, and W. F. Reed, “Angle-dependent effects in DLS measurements of polydisperse particles,” *Meas. Sci. Technol.* **33**(4), 045202 (2022).
- ⁴M. Kloczewiak, J. M. Banks, L. Jin, and M. L. Brader, “A biopharmaceutical perspective on higher-order structure and thermal stability of mRNA vaccines,” *Mol. Pharmaceutics* **19**(7), 2022–2031 (2022).
- ⁵J. L. Thelen, W. Leite, V. S. Urban, H. M. O'Neill, A. V. Grishaev, J. E. Curtis, S. Krueger, and M. M. Castellanos, “Morphological characterization of self-amplifying mRNA lipid nanoparticles,” *ACS Nano* **18**(2), 1464–1476 (2024).
- ⁶S. I. Abdel-Khalik and R. B. Bird, “Rheology of lopsided-dumbbell suspensions,” *Appl. Sci. Res.* **30**, 268–170 (1975).
- ⁷N. Phan-Thien, M. A. Kanso, and A. J. Giacomini, “Lopsided elastic dumbbell suspension,” *Phys. Fluids* **36**(7), 071707 (2024).
- ⁸N. Phan-Thien, D. Pan, M. A. Kanso, and A. J. Giacomini, “Lopsided rigid dumbbell rheology from Langevin equation: A graduate tutorial,” *Phys. Fluids* **36**(9), 091801 (2024).
- ⁹C. Malburet, L. Leclercq, J. F. Cotte, J. Thiebaud, E. Bazin, M. Garinot, and H. Cottet, “Size and charge characterization of lipid nanoparticles for mRNA vaccines,” *Anal. Chem.* **94**(11), 4677–4685 (2022).
- ¹⁰S. Li, U. Hu, A. Li, J. Lin, K. Hsieh, Z. Schneiderman, P. Zhang, Y. Zhu, C. Qiu, E. Kokkoli, and T. H. Wang, “Payload distribution and capacity of mRNA lipid nanoparticles,” *Nat. Commun.* **13**(1), 5561 (2022).
- ¹¹J. Whitley, C. Zwolinski, C. Denis, M. Maughan, L. Hayles, D. Clarke, M. Snare, H. Liao, S. Chiou, T. Marmura, and H. Zoeller, “Development of mRNA manufacturing for vaccines and therapeutics: MRNA platform requirements and development of a scalable production process to support early phase clinical trials,” *Transl. Res.* **242**, 38–55 (2022).
- ¹²L. Schoenmaker, D. Witzigmann, J. A. Kulkarni, R. Verbeke, G. Kersten, W. Jiskoot, and D. J. A. Crommelin, “mRNA-lipid nanoparticle COVID-19 vaccines: Structure and stability,” *Int. J. Pharm.* **601**, 120586 (2021).
- ¹³R. B. Bird, O. Hassager, R. C. Armstrong, and C. F. Curtiss, *Dynamics of Polymeric Liquids*, 1st ed. (Wiley, New York, 1977), Vol. 2.
- ¹⁴M. A. Kanso, J. H. Piette, J. A. Hanna, and A. J. Giacomini, “Coronavirus rotational diffusivity,” *Phys. Fluids* **32**(11), 113101 (2020).
- ¹⁵R. B. Bird, C. F. Curtiss, R. C. Armstrong, and O. Hassager, *Dynamics of Polymeric Liquids*, 2nd ed. (Wiley, New York, 1987), Vol. 2.
- ¹⁶R. Chakraborty, D. Singhal, M. A. Kanso, and A. J. Giacomini, “Macromolecular complex viscosity from space-filling equilibrium structure,” *Phys. Fluids* **34**(9), 093109 (2022).
- ¹⁷M. A. Kanso and A. J. Giacomini, “General rigid bead-rod macromolecular theory,” in *Recent Advances in Rheology: Theory, Biorheology, Suspension and Interfacial Rheology*, 1st ed., edited by D. D. Kee and A. Ramachandran (AIP Publishing, Melville, NY, 2022), Chapter 2, pp. 2–1–2–32. Errata: Below Eq. (2.78), “...increases with N ” should be “...increases with N^3 ”. Above Eq. (2.80), “(77)” should be “(2.77).”

- ¹⁸J. H. Piette, L. M. Jbara, C. Saengow, and A. J. Giacomini, "Exact coefficients for rigid dumbbell suspensions for steady shear flow material function expansions," *Phys. Fluids* **31**(2), 021212 (2019). Erratum: Above Eq. (83), "one other" should be "one other use"; below Eq. (8), "descend the" should be "descend with."
- ¹⁹D. C. Evans, H. R. Warner, Jr., W. R. Ramakka, and R. B. Bird, "Behavior of solutions of linear macromolecules in steady shear flow with superposed oscillations," *J. Chem. Phys.* **52**, 4086–4089 (1970).
- ²⁰R. B. Bird, A. J. Giacomini, A. M. Schmalzer, and C. Aumtate, "Dilute rigid dumbbell suspensions in large-amplitude oscillatory shear flow: shear stress response," *J. Chem. Phys.* **140**(7), 074904–074916 (2014). pp 1-Errata: Ganged after Ref. 116 of Ref. 21 below.
- ²¹C. Saengow, A. J. Giacomini, and C. Kolitawong, "Exact analytical solution for large-amplitude oscillatory shear flow from Oldroyd 8-constant framework: Shear stress," *Phys. Fluids* **29**(4), 043101 (2017). Errata: In column 4 of rows 12 and 13 of TABLE IV, $\lambda_2 = \mu_0 = \mu_1$ should be $\mu_1 = -\lambda_1; \lambda_2 = \mu_0$ and $\mu_1 = \lambda_1; \lambda_2 = \mu_0$.
- ²²A. J. Giacomini, L. M. Jbara, and C. Saengow, "Pattern method for higher harmonics from macromolecular orientation in oscillatory shear flow," *Phys. Fluids* **32**(1), 011703 (2020).
- ²³A. J. Giacomini, L. M. Jbara, and C. Saengow, "Pattern method for higher harmonics of first normal stress difference from molecular orientation in oscillatory shear flow," *Phys. Fluids* **32**(3), 031704 (2020).
- ²⁴L. M. Jbara and A. J. Giacomini, "Orientation distribution function pattern for rigid dumbbell suspensions in any simple shear flow," *Macromol. Theory Simul.* **28**(1), 1800046 (2019).
- ²⁵L. M. Jbara, A. J. Giacomini, and P. H. Gilbert, "Macromolecular origins of fifth shear stress harmonic in large-amplitude oscillatory shear flow," *Nihon Reoriji Gakkaishi (J. Soc. Rheol., Jpn.)* **44**(5), 289–302 (2017). Errata: Ganged in Ref. 126 of Ref. 21 above; In the last row of Table II, "storage viscosity" should be "loss and storage viscosities."
- ²⁶R. B. Bird, H. R. Warner, Jr., and D. C. Evans, "Kinetic theory and rheology of dumbbell suspensions with brownian motion," *Adv. Polym. Sci.* **8**, 1–90 (1971). Erratum: After Eq. (5.1), "rotatory" should be "rotational".
- ²⁷R. B. Bird, D. C. Evans, and H. R. Warner, Jr., "Recoil in macromolecular solutions according to rigid dumbbell kinetic theory," *Appl. Sci. Res.* **22**, 185–192 (1970).
- ²⁸R. B. Bird and H. R. Warner, Jr., "Creep in macromolecular solutions according to rigid dumbbell kinetic theory," *Appl. Sci. Res.* **22**, 193–196 (1970).
- ²⁹M. C. Pak, A. J. Giacomini, and M. A. Kalso, "Steady elongational flow from rotator theory," *Phys. Fluids* **35**(10), 103116 (2023).
- ³⁰P. Pongthong, A. J. Giacomini, and C. Saengow, "Planar extensional viscosity from Oldroyd 8-constant framework," *Phys. Fluids* **36**(1), 017130 (2024).
- ³¹P. Pongthong and A. J. Giacomini, "Bridging macromolecular theory of polymeric liquids to Oldroyd 8-constant constitutive framework," *Phys. Fluids* **35**(11), 111705 (2023).
- ³²H. R. Warner, Jr. and R. B. Bird, "A molecular interpretation of the steady state Maxwell orthogonal rheometer flow," *AIChE J.* **16**, 150 (1970).
- ³³M. Brader and J. Banks, "Methylene blue stabilized mRNA compositions," U.S. patent application 17/926,353 (2023).
- ³⁴M. A. Kalso, A. J. Giacomini, C. Saengow, and J. H. Piette, "Macromolecular architecture and complex viscosity," *Phys. Fluids* **31**(8), 087107 (2019). Editor's pick. Errata: Ganged in Ref. 8 "of Ref. 35 below. In the caption to FIG. 1, "(rightmost)" should be "(leftmost)", and "(leftmost)" should be "(rightmost)".
- ³⁵M. A. Kalso, V. Chaurasia, E. Fried, and A. J. Giacomini, "Peplomer bulb shape and coronavirus rotational diffusivity," *Phys. Fluids*, **33** 33(3), 033115 (2021).
- ³⁶A. J. Giacomini, S. J. Coombs, M. C. Pak, and K-I. Kim, "General rigid bead-rod theory for steady-shear flow," *Phys. Fluids* **35**(8), 083111 (2023).
- ³⁷F. Jia, W. Huang, Y. Yin, Y. Jiang, Q. Yang, H. Huang, G. Nie, and H. Wang, "Stabilizing RNA nanovaccines with transformable hyaluronan dynamic hydrogel for durable cancer immunotherapy," *Adv. Funct. Mater.* **33**(3), 2204636 (2023).
- ³⁸T. C. Laurent and J. R. Fraser, "Hyaluronan," *Feder. Am. Soc. Exp. Biol.* **6**(7), 2397–2404 (1992).
- ³⁹S. de Chateaufort-Randon, B. Bresson, M. Ripoll, S. Huille, E. Barthel, and C. Monteux, "The mechanical properties of lipid nanoparticles depend on the type of biomacromolecule they are loaded with," *Nanoscale* **16**, 10706–10714 (2024).
- ⁴⁰ASTM D2240-15, *Standard Test Method for Rubber Property—Durometer Hardness* (ASTM International, West Conshohocken, PA, 2021).
- ⁴¹Mix, A. W. and A. J. Giacomini, "Standardized polymer durometry," *J. Test. Eval.* **39**(4), 1–10 (2011). Erratum: In TABLE 3, Y_c should be Y_c .
- ⁴²P. H. Gilbert and A. J. Giacomini, "Exact analytical durometer hardness scale interconversion," *J. Test. Eval.* **46**(5), 1995–2032 (2018). Errata: In Ref. 14, "Giacomini" should be "Giacomini"; after Eq. (1), "conical, and hemispherical" should be "hemispherical, and conical."
- ⁴³M. Hoffmann, Y. Lu, M. Schrunner, M. Ballauff, and L. Harnau, "Dumbbell-shaped polyelectrolyte brushes studied by depolarized dynamic light scattering," *J. Phys. Chem. B* **112**(47), 14843–14850 (2008).
- ⁴⁴J. H. Piette, C. Saengow, and A. J. Giacomini, "Hydrodynamic interaction for rigid dumbbell suspensions in steady shear flow," *Phys. Fluids* **31**(5), 053103 (2019).
- ⁴⁵M. C. Pak, K-I. Kim, M. A. Kalso, and A. J. Giacomini, "General rigid bead-rod theory with hydrodynamic interaction for polymer viscoelasticity," *Phys. Fluids* **34**(2), 023106 (2022).
- ⁴⁶M. A. Kalso, M. C. Pak, K-I. Kim, S. J. Coombs, and A. J. Giacomini, "Hydrodynamic interaction and complex viscosity of multi-bead rods," *Phys. Fluids* **34**(4), 043102 (2022).
- ⁴⁷P. H. Gilbert and A. J. Giacomini, "Molecular origins of higher harmonics in large-amplitude oscillatory shear flow: Shear stress response," *Phys. Fluids* **28**(10), 2016–2036 (2016). Erratum: In Eq. (D1), $\dot{\epsilon}_0$ should be $\dot{\gamma}_0$.
- ⁴⁸R. B. Bird and H. R. Warner, "Hydrodynamic interaction effects in rigid dumbbell suspensions. I. Kinetic theory," *Trans. Soc. Rheol.* **15**(4), 741–750 (1971).
- ⁴⁹J. H. Piette, C. Saengow, and A. J. Giacomini, "Zero-shear viscosity of Fraenkel dumbbell suspensions," *Phys. Fluids* **32**(6), 063103 (2020).
- ⁵⁰S. Kim and C. J. Lawrence, "Similarity solutions for the orientation distribution function and rheological properties of suspensions of axisymmetric particles with external couples," *J. Non-Newtonian Fluid Mech.* **24**(3), 297–310 (1987).
- ⁵¹W. Stasiak and C. Cohen, "Dilute solutions of macromolecules in a rectilinear Poiseuille flow," *J. Chem. Phys.* **78**(1), 553–559 (1983).
- ⁵²S. J. Coombs, K. Tontiwattanakul, and A. J. Giacomini, "Macromolecular microfluidic concentrators," *Phys. Fluids* **34**(10), 103115 (2022).
- ⁵³O. O. Park and G. G. Fuller, "Dynamics of rigid and flexible polymer chains in confined geometries. I. Steady simple shear flow," *J. Non-Newtonian Fluid Mech.* **15**, 309–329 (1984).
- ⁵⁴O. O. Park and G. G. Fuller, "Dynamics of rigid and flexible polymer chains in confined geometries. II. Time-dependent shear flow," *J. Non-Newtonian Fluid Mech.* **18**, 111–122 (1985).
- ⁵⁵O. O. Park, "Dynamics of rigid and flexible polymer chains," Ph.D. thesis (Stanford University, 1985).
- ⁵⁶S. J. Coombs, R. Pasquino, and A. J. Giacomini, "Confinement and complex viscosity," *Phys. Fluids* **33**(4), 053104 (2021).
- ⁵⁷H. Alimohamadi, H. E. W.-C. Luo, S. Gupta, J. de Anda, R. Yang, T. Mandal, and G. C. L. Wong, "Comparing multifunctional viral and eukaryotic proteins for generating scission necks in membranes," *ACS Nano* **18**(24), 15545–15556 (2024).
- ⁵⁸B. Peng, H. R. Vutukuri, A. van Blaaderen, and A. Imhof, "Synthesis of fluorescent monodisperse non-spherical dumbbell-like model colloids," *J. Mater. Chem.* **22**(41), 21893–21900 (2012).
- ⁵⁹J.-W. Kim, R. J. Larsen, and D. A. Weitz, "Synthesis of nonspherical colloidal particles with anisotropic properties," *J. Am. Chem. Soc.* **128**(44), 14374–14377 (2006).
- ⁶⁰A. Z. Mühlen, E. Z. Mühlen, H. Niehus, and W. Mehnert, "Atomic force microscopy studies of solid lipid nanoparticles," *Pharm. Res.* **13**, 1411–1416 (1996).
- ⁶¹Y. Takechi-Haraya, A. Usui, K. I. Izutsu, and Y. Abe, "Atomic force microscopic imaging of mRNA-lipid nanoparticles in aqueous medium," *J. Pharm. Sci.* **112**(3), 648–652 (2023).
- ⁶²Y. Takechi-Haraya, K. Sakai-Kato, Y. Abe, T. Kawanishi, T. H. Okuda, and Y. Goda, "Atomic force microscopic analysis of the effect of lipid composition on liposome membrane rigidity," *Langmuir* **32**(24), 6074–6082 (2016).

- ⁶³Y. Takechi-Haraya, Y. Goda, and K. Sakai-Kato, "Atomic force microscopy study on the stiffness of nanosized liposomes containing charged lipids," *Langmuir* **34**(26), 7805–7812 (2018).
- ⁶⁴N. Delorme and A. Fery, "Direct method to study membrane rigidity of small vesicles based on atomic force microscope force spectroscopy," *Phys. Rev. E* **74**(3), 030901 (2006).
- ⁶⁵E. Reissner, "Stresses and small displacements of shallow spherical shells. II," *J. Math. Phys.* **25**(1–4), 279–300 (1946).
- ⁶⁶S. L. Lee, T. F. O'Connor, X. Yang, C. N. Cruz, S. Chatterjee, R. D. Madurawe, C. M. Moore, X. Y. Lawrence, and R. D. Braatz, "Modernizing pharmaceutical manufacturing: From batch to continuous production," *J. Pharm. Innov.* **10**(3), 191–199 (2015).
- ⁶⁷R. Lakerveld, B. Benyahia, R. D. Braatz, and P. I. Barton, "Model-based design of a plant-wide control strategy for a continuous pharmaceutical plant," *AIChE. J.* **59**(10), 3671–3685 (2013).
- ⁶⁸S. Mascia, P. L. Heider, H. Zhang, R. Lakerveld, B. Benyahia, P. I. Barton, R. D. Braatz, C. L. Cooney, J. M. Evans, T. F. Jamison, and K. F. Jensen, "End-to-end continuous manufacturing of pharmaceuticals: Integrated synthesis, purification, and final dosage formation," *Angew. Chem.* **125**(47), 12585–12589 (2013).